Experimental and numerical analysis of a scaled dry-joint arch on moving supports

Abstract: This paper aims to investigate the response of a scaled segmental dry-joint masonry arch to the settlement of one support. An experimental test and numerical simulations were performed by applying incremental vertical displacements at the right support up to collapse. The experimental test was carried out on a 1:10 small-scale model of the arch made of bi-component composite blocks with dry joints. Numerical simulations were performed using a Finite Element (FE) micro-modelling approach, where the arch was discretized as a set of very stiff voussoirs connected by nonlinear interfaces. Experimental and numerical results were compared in terms of displacement capacity and collapse mechanisms. The sensitivity of the numerical results to the interface stiffness was also evaluated.

Keywords: masonry arches; experimental tests; FE micro-modelling; support displacements; collapse mechanisms; rigid blocks.

Reference to this paper should be made as follows: Author. (xxxx) 'Title', *Int. J. xxxxxxxxxx xxxxxxxxxx*,

1 Introduction

Arched structures are widespread in existing masonry buildings, especially historical constructions. It is well known that arches are very sensitive to any small change in the external environment; thus, they crack when subject to differential displacements of the abutments (Huerta, 2001). Although cracks are not dangerous a priori, they may become a source of concern when they are accompanied by large deformations.

Support movements can be induced by a range of causes including foundation settlements, leaning of supporting piers and walls, construction defects, soil heterogeneity, landslide, subsidence, etc. These phenomena are not instantaneous but can affect historic masonry structures for decades or even centuries, causing support displacements to increase significantly over time (Ochsendorf, 2006). As a result, arches can finally collapse if the progressive changes in the geometry produce sufficient cracks (idealized as hinges) to transform the structure into a mechanism (Heyman, 1966).

Several works recently investigated the response of masonry arches and vaults to support movements by means of analytical, numerical and experimental methods. Most of these studies described the mechanical behaviour of masonry materials using the simplified assumptions of (i) infinite compressive strength, (ii) no tensile strength and (iii) no sliding failure introduced by Heyman (1966; 1985). As a result, arches were modelled as assemblies of rigid blocks connected by no-tension friction interfaces.

Analytical methods were typically used for structures with a bi-dimensional behaviour, like arches and barrel vaults, since their application on three-dimensional structures, such as

cross vaults, is hardly feasible. In particular, different analytical methodologies were developed (i) to identify the position of the three hinges opening as soon as supports move (Como, 2016; Zampieri et al., 2018a, Galassi et al., 2018) as well as (ii) to predict the ultimate displacement capacity and collapse mechanisms for rigid-block arches with different geometries (e.g. Coccia et al., 2015; Ochsendorf, 2006; Smars, 2010; Zampieri et al., 2018b, Galassi et al., 2018; 2020). In the first case, the assumption of small displacements was used, whereas, in the second case, large displacements were considered due to the progressive changes in the geometry of the arch.

More in detail, Ochsendorf (2006) and Coccia et al. (2015) developed iterative procedures, respectively based on the static and kinematic approach of limit analysis, to determine the collapse displacement and corresponding horizontal thrust for circular arches on horizontal spreading supports. The same procedure proposed in Ochsendorf (2006) was applied by Romano and Ochsendorf (2010) for the analysis of pointed arches on spreading supports.

Zampieri et al. (2018a) and Galassi et al. (2018) proposed novel methodologies, the first combining the static and kinematic theorems of limit analysis, and the second based on combinatorial analysis coupled with static and kinematic procedures, to identify the position of the three initial hinges occurring in circular arches subject to horizontal, vertical and inclined support displacements. The same procedure proposed in Zampieri et al. (2018a) was adopted in Zampieri et al. (2019) to analyse an arch-pillar system with settling supports and was extended in Zampieri et al. (2018b) in the framework of large displacements. Galassi et al. (2018; 2020) extended their procedure in the large displacement regime to evaluate the collapse mechanisms and limit support displacements of circular and pointed arches.

In the framework of numerical methods, Discrete (or Distinct) Element models (DEM) were widely used to study the collapse of masonry arches and vaults due to support displacements (e.g. D'Altri et al., 2018; Foti et al., 2018; Lengyel, 2017; McInerney and DeJong, 2015; Van Mele et al., 2012). DE models offer the possibility of using rigid or quasi-rigid blocks and simulating large relative movements between the units (Lemos, 2007). As a result, they are particularly suitable to investigate collapse mechanisms due to loss of stability and progressive changes in the geometry, like those exhibited by arches and vaults.

Beyond DE models, FE models can also be used to evaluate the effects of large support displacements on masonry arches and vaults (e.g. Alforno et al., 2020, Masciotta et al., 2020, Zampieri et al., 2018a), provided that geometrical nonlinearities are properly considered. Nevertheless, FE methods have the drawback of becoming computationally demanding and extremely time consuming when dealing with large complicated structures. In particular, the application of FE micro-modelling on arched structures subject to support movements is very limited. Zampieri et al. (2018a) adopted a FE micro-modeling strategy to investigate the response of segmental masonry arches to vertical and inclined displacements of one support. Very recently, Alforno et al. (2020) proposed a simplified micro-modelling approach, based on the use of a commercial software, to analyse the structural behaviour of dry-joint masonry arches and vaults subject to support displacements and seismic actions.

Analytical and numerical predictions were often validated by comparison with the results from experimental tests performed on small-scale models of arches and vaults on moving

supports (e.g. Alforno et al., 2020; D'Altri et al., 2020; Galassi et al., 2018; 2020; Ochsendorf, 2006; Romano and Ochsendorf, 2010; Smars, 2010; Van Mele et al., 2012; Zampieri et al., 2018a). Major results report that the analytical and numerical methods generally overpredict the displacement capacity obtained experimentally due to the imperfections and inaccuracies that characterize the physical models compared to the "perfect" numerical ones. It is worth noting that, since testing full-scale models is particularly challenging, small-scale models were widely used to assess the stability of masonry arches and vaults, not only under support displacements, but also under seismic actions (e.g. Calderini et al., 2015; DeJong et al., 2008; Gaetani et al., 2017; Misseri et al., 2018; Rossi et al., 2016; Shapiro, 2012) and point loads (e.g. Pippard and Ashby, 1939; Shapiro, 2012). As proved by Heyman (1995), the stability of masonry structures depends on geometry rather than on material strength; thus, their behaviour can be considered independent on scale.

In this paper, the behaviour of a scaled segmental dry-joint masonry arch subject to the settlement of one support was investigated by means of a preliminary experimental test and numerical analyses. The geometry of the arch is consistent with the cross-section of barrel vaults typically used as ceiling in historic masonry churches. The experimental test was carried out on a 1:10 scaled model built as a dry-joint assembly of bi-component composite voussoirs. A monotonically increasing vertical displacement was applied at one support of the arch until reaching the collapse. Numerical analyses were performed using a FE micro-modelling strategy, where each voussoir was modelled as a distinct block and dry-joints were represented as no-tension friction interfaces. A sensitivity analysis to the interface stiffness was also performed.

The aims of the work were to (i) identify the collapse mechanism of the segmental arch under vertical displacement loading, (ii) determine the maximum displacement capacity at collapse, and (iii) assess the capacity of the numerical model to predict experimental results. It is important to highlight that this paper aims to present the preliminary results of a single experimental test and corresponding numerical simulations. Within the framework of a larger research project aimed at assessing the structural behaviour of masonry arches on moving supports, further experimental tests will be carried out by analysing different configuration of support displacements (vertical, horizontal and diagonal). Nevertheless, this paper already presents some aspects of novelty. Firstly, the arch discretization in voussoirs reproduces almost realistically the size, shape and arrangement of the units of a real brick masonry arch. This is the main difference with respect to the physical models of dry-joint masonry arches tested so far under vertical support displacements (Galassi et al., 2018; Romano and Ochsendorf, 2010; Smars, 2020). Secondly, the FE micro-modelling strategy proposed here allows simulating the experimental response of masonry arches on moving supports by considering the actual deformability of contact surfaces. The effect of the imperfections that characterize masonry arches is typically taken into account in numerical simulations by reducing arch thickness (e.g. Albuerne et al., 2013; DeJong et al., 2008; Gaetani, 2016). Differently, in this work the numerical results are tuned with the experimental evidences by properly setting the stiffness of the interface elements.

Author

2 Experimental test

2.1 Physical model and testing set-up

The test was performed on a 1:10 small scale model of a segmental dry-joint arch supported by two piers. The arch geometry was defined taking as reference the standard cross-section of the barrel vaults that are typically used as ceiling in the main nave of historic masonry churches. In particular, a barrel vault made of two layers of standard bricks (radial thickness of 0.24 m) and having a net span of 6 m was considered. This type of vaults generally does not have any backfill, but it is merged with the supporting walls at the abutments. For this reason, the springings of the physical model were considered at about 27° from the horizontal plane.

The geometry of the mockup is shown in Figure 1. The arch has an angle of embrace of 125°, an internal radius of 300 mm, a net span of 533 mm, a radial thickness of 24 mm and a depth of 120 mm. It is composed of 55 voussoirs with a height of 24 mm and a width of about 12 mm, representing the scaled dimensions of two adjacent bricks of standard size (60x120x240 mm^3) positioned with their longest side along the radial plane. Reproducing exactly the real pattern of a two-course brick barrel vault would have requested the production of extremely small voussoirs, making their assembly very complicated. The shape of the blocks is slightly trapezoidal in order to compensate the lack of mortar between them. The choice to model the arch as a dry-joint assembly of blocks gives the chance to repeat different series of tests using the same units and reduces significantly the time needed for the set-up of the physical model. Furthermore, neglecting mortar joints is consistent with the assumption of no tensile strength usually adopted for masonry materials (see Heyman, 1985).

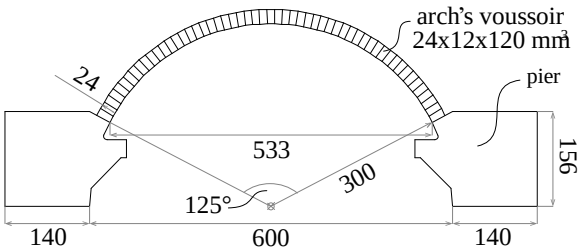

Figure 1: Geometry of the arch mockup (in mm).

The arch is supported by two piers with a height of 156 mm and a width of 140 mm, shaped in such a way that they can sustain the plywood scaffolding needed to build the arch (Figure 2a). As shown in Figure 2b, the blocks of the piers are designed as a sort of Lego system, allowing to add parallelepiped blocks above and below. This technique will enable to test more complex arch-pillar systems in future experimental campaigns.

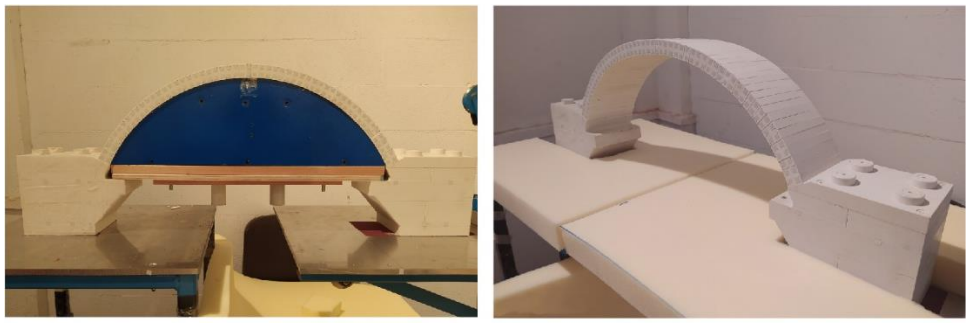

a) b)

Figure 2: Physical model: a) plywood scaffolding, b) view after the removal of the scaffolding.

All the blocks (voussoirs and piers) are made of a bi-component composite material, which was poured, let it dry and then removed from special silicone moulds (Figure 3). The use of this technique to create blocks is an innovation in the framework of the tests performed on small-scale models, which often employ 3D printed plastic blocks (e.g. Rossi et al., 2016; Rossi et al., 2017; Barentin et a., 2017). This technique allows to significantly reduce the cost of building models and, in addition, it enables to re-create easily new blocks as soon as they are needed, directly in the laboratory.

The bi-component composite material is made by mixing a mineral powder with an acrylic polymer in aqueous solution. This material offers several advantages over other grouts traditionally used for small-scale models, such as cast concrete (e.g. Ochsendorf, 2006; Romano and Ochsendorf, 2010): (i) it allows producing very small blocks with high dimensional accuracy, (ii) it is easy to mix, even manually, without requiring any special equipment, (iii) it hardens very fast and can be demoulded approximately one hour after the pouring and (iv) it does not experience any appreciable shrinkage. The composite material has a density and a friction angle of about 1.64 g/cm^3 and 41.2°, respectively. The friction angle was measured by testing 10 couples of blocks on an inclined plane. The material compressive strength and Young's modulus are 9.1 MPa and 941 MPa, respectively. They were evaluated by conducting compressive tests on parallelepiped specimens in the Structural and Material Laboratory of the University of Genoa (Figure 4).

Author

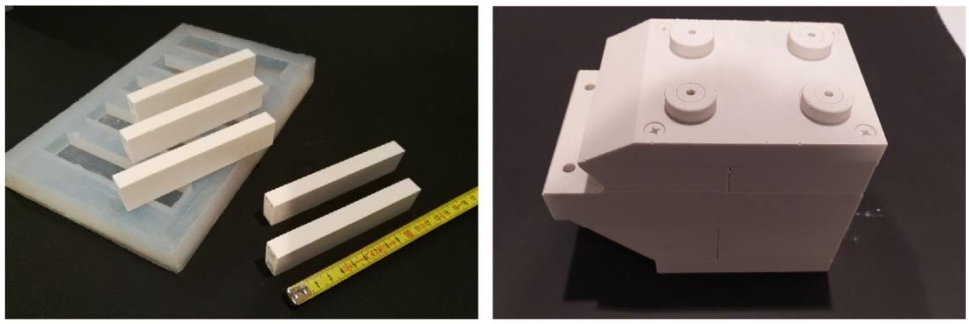

a) b)

Figure 3: Bi-component composite blocks: a) arch voussoirs and silicone mould used for their production, b) pier.

Figure 4: Compressive tests to characterize the bi-component composite material used for the blocks.

The experimental test was performed by applying an increasing vertical displacement δ at the right support of the arch. The displacement was applied in a quasi-static way (velocity of 0.23 mm/s) by means of an external stepper motor linear actuator controlled via software (Figure 5a). The development of the mechanism up to collapse was recorded through a high frame rate (60 Hz) and high-resolution camera (Figure 5b).

a) b)

Figure 5: a) Testing machine, b) high frame rate and high-resolution camera.

2.2 Results

The results of the experimental test are presented here in terms of damage mechanisms and displacement capacity. The evolution of the damage of the arch with the increasing applied vertical displacement δ is shown in Figure 6. As shown in Figure 6a, two hinges (B and C) are initially formed at the extrados, one located between 31th and 32th blocks and the other one placed at the right support. Then, as the vertical displacement δ increases, a third hinge (A) occurs at the intrados between 11th and 12th blocks (Figure 6b). As shown in Figure 6c, an asymmetrical four-hinge mechanism is obtained for an applied vertical displacement of 48.9 mm. In particular, it is observed that hinge A moves one block towards the crown and a fourth hinge (D) appears at the left support. As shown in Figure 6, the occurrence of a fourth hinge triggers the collapse leading the arch to deform like an assembly of three rigid blocks (denoted as block 1, 2 and 3 from left to right) rotating around four hinges. It is interesting to observe that block 3 rotates upwards with increasing vertical displacement up to the opening of hinge D. Then, as shown in Figure 6d, as soon as hinge D is formed, block 1 starts to rotate upwards, while block 3 starts to rotate downwards. It is also observed that, for rigid-block kinematics, the downward rotation of block 3 requires the closure of hinge C at the extrados as well as the opening of a new opposite hinge at the intrados (Figure 6d).

Author

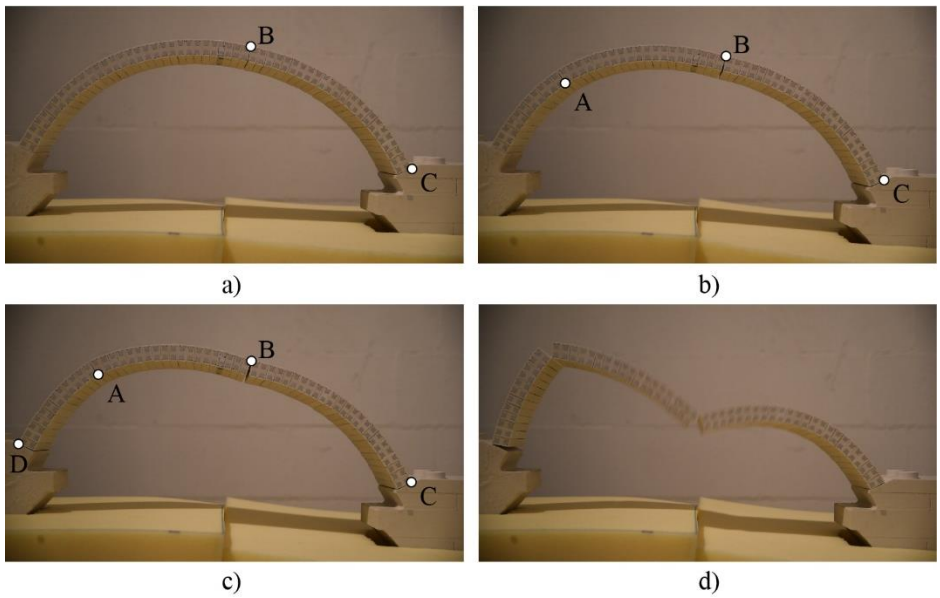

Figure 6: Damage mechanisms obtained in the physical test for an applied vertical displacement δ of a) 21.9 mm, b) 38.1 mm, c) 48.9 mm and d) 48.9 mm.

3 Finite Element Micro-Modelling

3.1 Description of the numerical model

The response of the arch to the vertical displacement of one support was simulated computationally using the FEM software DIANA (TNO DIANA, 2014). A 2D finite element model of the arch was created in Midas FX+ Version 3.3.0 (Customized Pre/Post-processor for DIANA software, FX+ for DIANA, 2013) adopting a micro-modelling approach. In particular, the arch was discretized as a set of very stiff and infinitely resistant in compression voussoirs connected by non-linear interfaces (Figure 7). This modelling approach is particularly suitable to simulate the experimental test since the physical model was created as an assembly of blocks with dry joints. Further interface elements were placed at the springing of the arch to allow for hinge opening. The piers were not included in the FE model, since they simply provided support to the arch.

The voussoirs were modelled by means of four-node quadrilateral isoparametric plane stress elements (Q8MEM), while the interfaces were modelled adopting 2D four-node line interface elements (L8IF). A mesh size of 2 mm (that is 12 elements along the thickness of the arch) was adopted based on a sensitivity analysis on the collapse displacement δ_u obtained by applying an increasing vertical displacement δ at the right support of the arch (Table 1). From Table 1, it is interesting to observe that almost the same displacement capacity was obtained regardless of the mesh size considered.

Table 1: Mesh sensitivity analysis (selected mesh size highlighted in bold).

Mesh size [mm]	Nr. of elements along the radial thickness	Collapse displacement δ_u [mm]	Computational time* [min]
4	6	21.2	≈ 3
3	8	21.2	≈ 12
2	**12**	**21.1**	**≈ 24**
1	24	21.1	≈ 52

* Intel® Core™ i7-8086K (4.00 GHz), RAM 32 GB, SSD disk

Figure 7 presents the FE micro-model of the arch, composed of 5031 nodes and 4632 elements. Pinned boundary conditions were assumed at the springings of the arch.

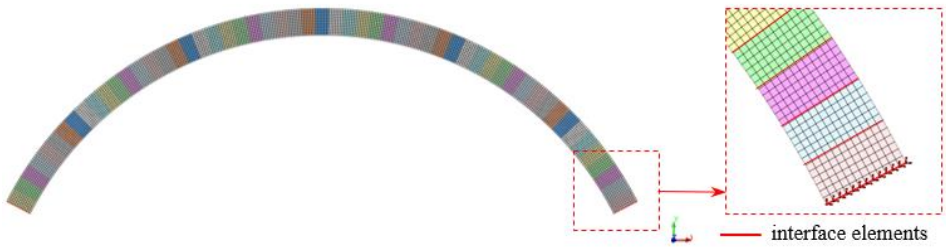

Figure 7: FE micro-model of the arch.

The voussoirs were modelled as linear elastic elements with infinite compressive strength. A Young's modulus of 941 MPa and a density of 1.64 gr/cm^3 were adopted, as measured for the material of the blocks of the physical model (see section 2). A Poisson's ratio equal to 0.2 was assumed. For interface elements, a Coulomb friction model was adopted. Cohesion and dilatancy angle were set equal to zero, while a friction angle of 41.2° was assumed, as measured for the material of the physical model. The friction criterion was extended with a gap criterion (TNO DIANA, 2014) with zero tensile strength in order to simulate hinge opening. In this way, a gap was assumed to open as soon as tensile stresses arose. For further details about the Coulomb friction model, the reader is referred to TNO DIANA (2014).

The response of the arch to displacement loading was investigated by means of non-linear static analyses. Firstly, the self-weight was applied, then the vertical displacement applied at the right support was increased monotonically until reaching the collapse. A regular Newton-Raphson iteration method in combination with a line search algorithm was adopted in the analyses (TNO DIANA, 2014). An energy-based convergence criterion with a tolerance value of 0.001 was assumed. Geometrical non-linearities were also taken into account adopting the Total Lagrange formulation available in DIANA (TNO DIANA, 2014).

3.1 Sensitivity analysis to interface stiffness

A sensitivity analysis was carried out to evaluate the effect of the interface stiffness on the arch response. Results from literature (e.g. Gaetani et al., 2017; Lourenço et al., 2010) have actually demonstrated that the interface stiffness plays an important role in the numerical assessment of masonry arches. A range of values between 0.1 and 100 N/mm^3 was adopted for the interface normal stiffness k_n according to the values used in the literature (Gaetani et al., 2017). The ratio between normal and tangential stiffness was set equal to 2 in order to optimize numerical convergence. In fact, although this ratio does not affect the structural response of the arch, it strongly influences the convergence of the numerical analyses.

Figure 8 shows the variation of the collapse displacement δ_u with the interface normal stiffness k_n. It is observed that the collapse displacement increases with increasing stiffness until reaching a maximum constant value that is not affected by any further stiffness increase.

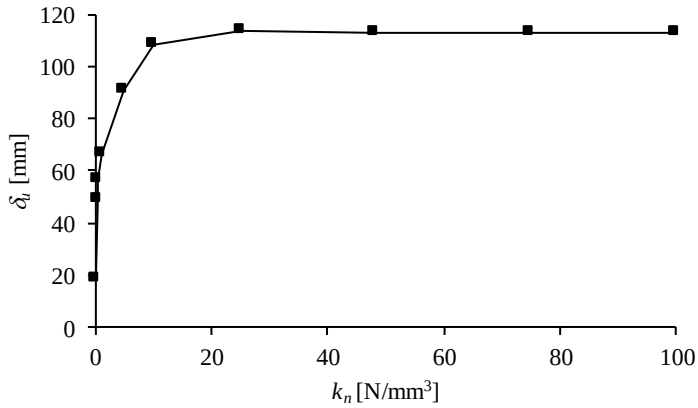

Figure 8: Collapse displacement δ_u vs. interface normal stiffness k_n.

A four-hinge collapse mechanism with hinges located in the sequence E-I-E-E (from left to right, where E = extrados; I = intrados) is predicted by FE analyses for any value of k_n (Figure 9a-b-c-d). When the right support starts to settle, three hinges, A, B and C, occur. Hinge A is located at the intrados at the haunches, whereas the consecutive hinges B and C appear at the extrados, respectively close to the crown and at the right support. Collapse is reached when a fourth hinge (D) appears at the left support at the extrados.

Figure 9 shows how the interface stiffness strongly influences the arch behavior in terms of deformed configuration. For very small values of k_n (Figure 9a), the arch does not behave as an assembly of rigid blocks, as typically observed for rigid-no tension structures. Conversely, it accommodates support displacements mainly thanks to its elastic deformability. As shown in Figure 9a, hinges are actually distributed among several adjacent interfaces. Furthermore, large interpenetration between the blocks occurs, causing hinges to move inward with respect to the intrados and extrados line, as already observed by Gaetani et al. 2017. This effect reduces the arch thickness and, consequently, results in a lower displacement capacity. As larger values of k_n are adopted (Figure 9b), hinges tend to concentrate in one or few interfaces, and the interpenetration between the blocks

decreases, with the result that the displacement capacity increases. For values of k_n falling within the plateau of the collapse displacement-interface normal stiffness curve (k_n equal or larger than approximately 10 N/mm^3) (Figure 9c-d), the arch behaves as an assembly of rigid blocks rotating around well-defined hinges. All the four hinges A, B, C and D open in one single interface. Furthermore, compressive stresses are concentrated in one single FE of the interfaces, indicating that hinges occur at the edge line of the arch.

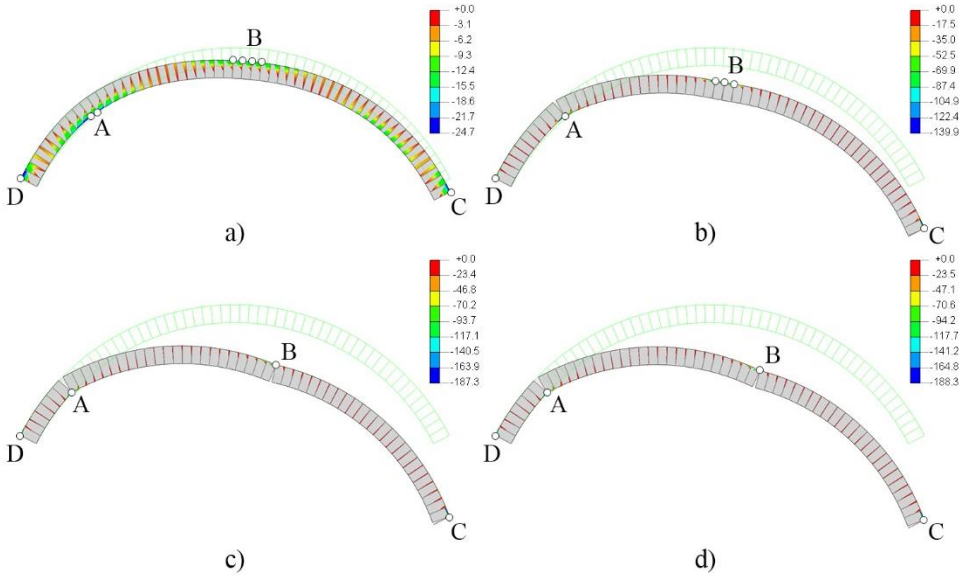

Figure 9: Collapse mechanism for different values of the interface normal stiffness, k_n: a) 0.1 N/mm^3 (δ_u = 18.0 mm), b) 1 N/mm^3 (δ_u = 66.7 mm), c) 10 N/mm^3 (δ_u = 108.6 mm), d) 100 N/mm^3 (δ_u = 113.1 mm) (results presented in terms of compressive stresses in the interfaces).

Figure 10 depicts the position of the hinges A, B, C and D as a function of the interface normal stiffness k_n. The interfaces where hinges appear are numbered from left to right, being interface no. 1 the interface at the left support. From Figure 10, it is easy to observe that, as k_n increases, hinges A and B, which are distributed among adjacent interfaces for low values of k_n, tend to concentrate in one single interface.

Figure 10 shows that the interface stiffness affects the arch response not only in terms of deformed shape, but also in terms of hinge position. As k_n increases, hinge A moves gradually towards the left support, whereas hinge B appears closer to the right support. However, the location of hinge A is the same for every value of k_n falling within the plateau region of the collapse displacement-interface normal stiffness curve. In the case of hinge B, its location does not change for k_n equal or larger than 48 N/mm^3.

Author

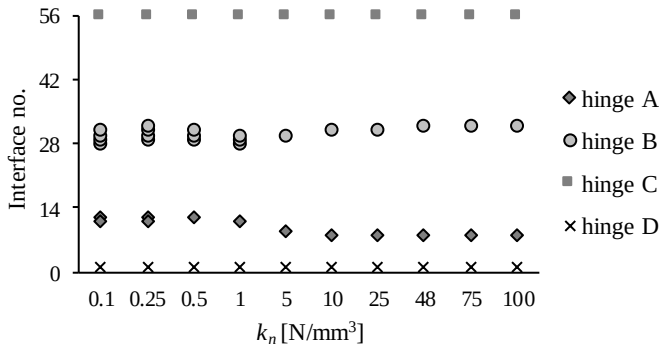

Figure 10: Hinge position as a function of the interface normal stiffness k_n.

3.2 Results and comparison with experimental test

Based on the results reported in section 3.1, the predictions of FE analyses are here compared to the experimental outcomes for two different values of interface stiffness: (i) a very large stiffness value (48 N/mm^3), chosen in the plateau region of the collapse displacement-interface normal stiffness curve (Figure 8), and (ii) a reduced stiffness value (0.25 N/mm^3), chosen so that the numerical collapse displacement matched the experimental result. The first value of k_n (48 N/mm^3) simulates rigid contact surfaces and, thus, allows to treat the arch as a rigid no-tension structure, whereas the second value (0.25 N/mm^3) enables to account for the imperfections (and resulting deformability) that may characterize the contact surfaces of the physical model.

The collapse mechanisms obtained from FE analyses for k_n equal to 48 N/mm^3 and k_n equal to 0.25 N/mm^3 are shown in Figure 11a and Figure 11b, respectively. For either value of k_n, the failure mode obtained numerically is the same as the experimental one, since collapse is governed by a four-hinge mechanism with hinges following the sequence E-I-E-E. It is worth noting that the numerical simulation stopped as soon as the fourth hinge appeared; thus, the collapse mechanism obtained numerically should be compared to the damage mechanism obtained in the experimental test before block 1 starts to rotate upwards (Figure 6).

For k_n equal to 48 N/mm^3 (Figure 11a), the arch behaves as an assembly of three rigid blocks rotating around four hinges, as observed for the physical model. The predicted position of hinges B, C and D is in full accordance with the experimental test, since hinge B appears between 31st and 32nd blocks (interface no. 32), and hinges C and D open at the supports. Conversely, hinge A appears five blocks closer to the left support with respect to the physical model. Although numerical and experimental results compare quite well in terms of collapse mechanism, the numerical simulations predict a collapse displacement δ_u of 112.6 mm, which is significantly higher than the experimental result (48.9 mm).

Reduced values of interface stiffness allow to predict a displacement capacity very similar to the experimental one. For k_n equal to 0.25 N/mm^3 (Figure 11b), a collapse displacement δ_u of 48.8 mm is obtained, which is almost equal to the experimental result (48.9 mm). The predicted hinge position is in better agreement with the experimental results with respect

to the FE simulation performed for k_n equal to 48 N/mm^3. Not only hinges B, C and D appear at the same location of the physical model, but also hinge A is shifted by one voussoir only with respect to the experimental test (the difference is of five voussoirs for k_n = 48 N/mm^3). Despite the very good agreement in terms of displacement capacity and hinge position, the numerical analyses performed for reduced values of stiffness do not capture accurately the actual behaviour of the physical model. In the FE model hinges A and B are distributed over adjacent interfaces, while in the experimental tests they concentrate in one single interface.

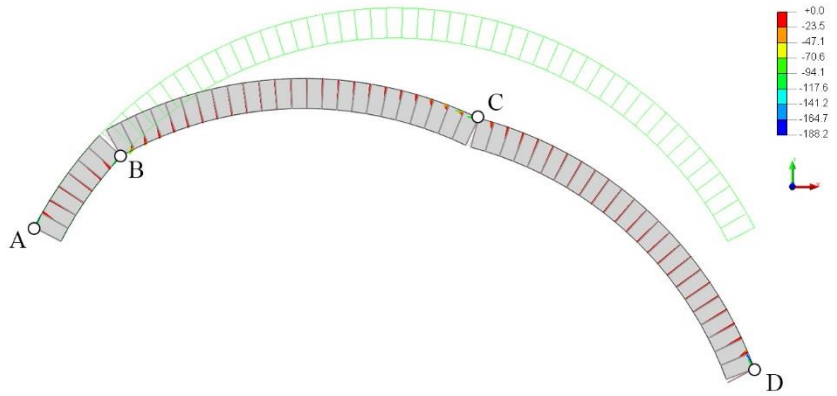

a)

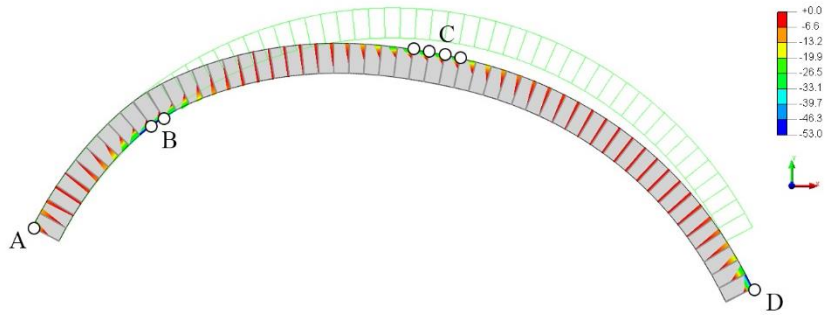

b)

Figure 11: Collapse mechanisms obtained from numerical analysis for a) k_n = 48.0 N/mm^3 (δ_u = 112.6 mm) and b) k_n = 0.25 N/mm^3 (δ_u = 48.8 mm) (results presented in terms of compressive stresses in the interfaces).

4 Conclusions

This paper presents the preliminary results of an experimental test and numerical simulations carried out on a segmental dry-joint masonry arch subjected to the settlement of one support. The test was performed on a 1:10 small-scale model made of bi-component composite blocks with dry joints. In order to appropriately simulate the experimental test, a micro-modelling approach was adopted in the numerical simulations, and the arch was

modelled as an assembly of very stiff voussoirs connected by nonlinear interfaces. The effect of the interface stiffness on the arch response was also evaluated.

Both the experimental test and the numerical analyses predict the occurrence of a four-hinge collapse mechanism with hinges located according to the sequence E-I-E-E. Nevertheless, the interface stiffness is found to have a significant influence on the numerical results in terms of collapse displacement, deformed configuration and hinge position. When very large values of interface stiffness are used, the numerical simulations predict a significantly larger collapse displacement compared to the experimental result. A discrepancy in terms of hinge position is also obtained. Conversely, reduced values of interface stiffness allow to obtain the same displacement capacity of the experimental test as well as a very good agreement in terms of hinge position, although hinges are more distributed with respect to the physical model. The not perfect agreement between the experimental test and the numerical simulation carried out for reduced values of interface stiffness may be attributed to some imperfections in the geometry assembled manually, which can be slightly different from that of the numerical model.

Based on these results, the reduced displacement capacity of the physical scale model compared to the "perfect" numerical model with very stiff interfaces can be reasonably attributed to the deformability of the contact surfaces of adjacent blocks. Such deformability is likely to be the consequence of both the roughness of contact surfaces and assembly inaccuracies. In this work, this effect is amplified by the large number of "imperfect and rough" interfaces (i.e. 57) present in the small-scale model investigated.

In conclusion, this work provides a contribution to the understanding of the structural response of dry-joint masonry arches subject to differential support displacements. In particular, the authors would like to stress that, although masonry structures are usually treated as assemblies of rigid blocks with no tension interfaces, greater attention should be paid to the deformability of the interfaces when considering displacement loading.

Future works will include a wide set of laboratory tests carried out by applying various configurations of differential support displacements (vertical, horizontal and diagonal). The effect of support movements on an arch-pillar system will be also analysed. Results will be provided not only in terms of ultimate displacement capacity, but also in terms of base reactions thanks to the implementation of a system of load cells able to measure both the vertical and horizontal reactions at the base of the physical models.

Acknowledgements.

References

Alforno, M., Venuti, F. and Calderini C. (2020) 'Validation of Simplified Micro-models for the Static Analysis of Masonry Arches and Vaults', *International Journal of Architectural Heritage*.

Albuerne, A, Williams, M and Lawson V. (2013) 'Prediction of the failure mechanism of arches under base motion using DEM based on the NSCD method', Wiadomości Konserw, Vol. 34, pp. 41–47.

Calderini, C., Lagomarsino, S., Rossi, M., De Canio, G., Mongelli, M.L. and Roselli, I. (2015) 'Shaking table tests of an arch-pillars system and design of strengthening by the use of tie-rods', *Bulletin of Earthquake Engineering*, Vol. 13, No. 1, pp. 279–297.

Barentin C., Van Mele, T. and Block, P. (2017) 'Robotically controlled scale-model testing of masonry vault collapse', *Meccanica*, Vol. 53, pp. 1917–1929.

Coccia, S., Di Carlo, F. and Rinaldi, Z. (2015) 'Collapse displacements for a mechanism of spreading-induced supports in a masonry arch', *International Journal of Advanced Structural Engineering*, Vol. 7 No. 3, pp. 307-320.

Como, M. (2016) *Statics of historic masonry constructions*, Springer International Publishing Switzerland.

D'Altri, A.M., De Miranda, S., Castellazzi, G., Sarhosis, V., Hudson, J. & Theodossopoulos, D. (2020) 'Historic barrel vaults undergoing differential settlements', *International Journal of Architectural Heritage*, Vol. 14 No. 8, pp.1196-1209.

DeJong, M., De Lorenzis L., Adams, S. and Ochsendorf J.A. (2008) 'Rocking stability of masonry arches in seismic regions', *Earthquake Spectra*, Vol. 2, pp. 847–865.

Foti, D., Vacca, V. and Facchini, I. (2018) 'DEM modeling and experimental analysis of the static behavior of a dry-joints masonry cross vaults', *Construction and Building Materials*, Vol. 170, pp. 111–120.

FX+ for DIANA. Midas FX+ for DIANA (2013) *Customized Pre/Post-processor for DIANA*.

Galassi, S., Misseri, G., Rovero, L. and Tempesta, G. (2018) 'Failure modes prediction of masonry voussoir arches on moving supports', *Engineering Structures*, Vol. 173, pp. 706-717.

Galassi, S., Misseri, G., Rovero, L. and Tempesta, G. (2020) 'Analysis of Masonry Pointed Arches on Moving Supports: A Numeric Predictive Model and Experimental Evaluations' in *Proceedings of XXIV AIMETA Conference 2019*, pp. 1-21.

Gaetani A. (2016) *Seismic Performance of Masonry Cross Vaults: Learning from Historical Developments and Experimental Testing*. PhD thesis, University of Minho, Guimarães, Portugal - Sapienza Università di Roma, Rome, Italy.

Gaetani, A., Lourenço P. B., Monti, G. and Moroni, M. (2017) 'Shaking table tests and numerical analyses on a scaled dry-joint arch undergoing windowed sine pulses', *Bulletin of Earthquake Engineering*, Vol. 15, pp. 4939-4961.

Heyman, J. (1966) 'The stone skeleton', *International Journal of Solids and Structures*, Vol. 2 No. 2, pp. 249-279.

Heyman, J. (1995) *The stone skeleton. Structural engineering of masonry architecture*, Cambridge University Press, Cambridge.

Huerta, S. (2001) 'Mechanics of masonry vaults: The equilibrium approach', Historical Constructions. Possibilities of numerical and experimental techniques, pp. 47-69.

Lemos, J. V. (2007) 'Discrete Element Modeling of Masonry Structures', *International Journal of Architectural Heritage*, Vol. 1, No. 2, pp. 190-213.

Lengyel, G. (2017) 'Discrete element analysis of gothic masonry vaults for self-weight and horizontal support displacement', Engineering Structures, Vol. 148, pp. 195–209.

Lourenço, P. B., Hunegn, T., Medeiros, P. and Peixinho, N. (2010), 'Testing and analysis of masonry arches subjected to impact loads' in *ARCH'10: Proceedings of the 6th International Conference on Arch Bridges*, Fuzhou University, China, pp. 603-610.

Masciotta, M-G., Pellegrini D, Girardi M, Padovani C, Barontini, A., Lourenço, P.B., Brigante D. and Fabbrocino G. (2020) 'Dynamic characterization of progressively damaged segmental masonry arches with one settled support: experimental and numericala analyses', *Frattura ed Integrità Strutturale*, Vol. 51. pp. 423-441.

McInerney, J. and DeJong, M.J. (2015) 'Discrete Element Modeling of Groin Vault Displacement Capacity', *International Journal of Architectural Heritage*, Vol. 9 No. 8, pp. 1037–1049.

Misseri, G., DeJong, M.J, and Rovero, L. (2018) 'Experimental and numerical investigation of the collapse of pointed masonry arches under quasi-static horizontal loading', *Engineering Structures*, Vol. 173, pp. 180-190.

Ochsendorf, J.A. (2006) 'The masonry arch on spreading supports', *Structural Engineer*, Vol. 84 No. 2, pp. 29-35.

Pippard A.J.S. and Ashby, R. (1939) 'An experimental study of the voussoir arch', *Journal of the Institution of Civil Engineers*, Vol. 10, No. 3, pp. 383-404.

Romano, A. and Ochsendorf, J.A. (2010) 'The mechanics of Gothic masonry arches', *International Journal of Architectural Heritage*, Vol. 4 No. 1, pp. 59-82.

Rossi, M., Calderini, C. and Lagomarsino, S. (2016) 'Experimental testing of the seismic in-plane displacement capacity of masonry cross vaults through a scale model', *Bulletin of Earthquake Engineering*, Vol. 14 No. 1, pp. 261-281.

Rossi, M., Calvo, Barentin C., Van Mele, T. and Block, P. (2017) 'Experimental study on the behaviour of masonry pavilion vaults on spreading supports', *Structures*, Vol. 11, pp. 110-120.

Shapiro E.E. (2012) *Collapse mechanism of small-scale unreinforced masonry vaults*. M.S. thesis in Building Technology, Massachusetts Institute of Technology.

Smars, P. (2010) 'Kinematic Stability of Masonry Arches', *Advanced Materials Research*, Vols. 133-134, pp. 429-434.

Van Mele, T., McInerney, J., DeJong, M. and Block P. (2012) 'Physical and Computational Discrete Modelling of Masonry Vault Collapse,' in *SAHC2012: Proceedings of 8th International Conference on Structural Analysis of Historical Constructions, Wroclaw, Poland*, pp. 2552–2560.

TNO DIANA BV. DIANA (2014) *Finite Element Analysis User's Manual Release 9.6*, Delft, The Netherlands.

Zampieri, P., Faleschini, F., Zanini, M.A., and Simoncello N. (2018a) 'Collapse mechanisms of masonry arches with settled springing', *Engineering Structures*, Vol. 156, pp. 363–74.

Zampieri, P., Simoncello, N. and Pellegrino, C. (2018b) 'Structural behaviour of masonry arch with no-horizontal springing settlement', *Frattura ed Integrità Strutturale*, Vol. 12 No. 43, pp. 182-190.

Zampieri, P., Amoroso, M. and Pellegrino, C. (2019) 'The masonry buttressed arch on spreading support', *Structures*, Vol. 20, pp. 226–236.